FINITE-SIZE SCALING FOR THE U(1) LATTICE GAUGE MODEL IN (2+1) DIMENSIONS

C. J. Hamer [1], K. C. Wang [1] and P. F. Price [2]
[1] *School of Physics,*
The University of New South Wales,
P.O. Box 1, Kensington, NSW 2033, Australia.
[2] *Computer Sciences Lab, RSPhy SE,*
Australian National University,
P.O. Box 4, Canberra, ACT 2601, Australia.
(March, 1993)

Abstract

The finite-size scaling behaviour of the compact U(1) lattice gauge model in two space and one time dimensions is studied using a Green's Function Monte Carlo method. The results agree with the predictions of effective Lagrangian theory and weak-coupling perturbation theory.

I. INTRODUCTION

The effective Lagrangian approach of Leutwyler, Hasenfratz and collaborators [1-3] has shed new light on the finite-size scaling properties of lattice systems in more than two dimensions. In particular, a system possessing a global continuous symmetry which undergoes spontaneous breakdown will develop Goldstone bosons, and the massless Goldstone bosons then control the response of the system to changes at low energies or temperatures, and large distances. One may write down an effective Lagrangian for the Goldstone bosons, and hence obtain a systematic large-volume expansion which gives universal formulae for the leading finite-size corrections in the theory. Conversely, measurement of the finite-size corrections can give estimates for the parameters of the effective Lagrangian.

In a recent paper [4], herafter referred to as I, a similar approach was applied to the Hamiltonian version of compact U(1) lattice gauge theory. Here the U(1) gauge symmetry is local rather than global, and there are no Goldstone bosons in the usual sense. The theory may, however, possess massless particles, namely the photons; and these might again be expected to control the large distance behaviour. In reference I, the leading term of the effective Lagrangian was taken to be simply that of free electromagnetic theory, and the finite-size scaling behaviour was predicted on that basis. Simple dimensional arguments show that any interactions between the photons must be "soft" at low energy, which again allows a systematic large-volume expansion. This was previously remarked by Kovner, Rosenstein and Eliezer [5], in fact, who argued that the photon could itself be regarded as a Goldstone boson, arising from spontaneous breakdown of a global symmetry generated by the magnetic flux[1]. A complementary weak-coupling perturbation analysis was also carried out in I, which predicted similar finite-size scaling behaviour, and also gave an expression for the photon velocity (i.e. the speed of light), which appears as an unknown parameter in the effective theory. The results were tested against Monte Carlo measurements [6] in the massless, Coulomb phase of the $(3+1)$ D model, and were found to be correct.

A more interesting question is whether the results can also be applied to the (2+1) D model, because that model **has** no massless phase. Göpfert and Mack [7] have proved that the model remains confining at all couplings, and that in the continuum limit it reduces to a theory of free, **massive** bosons, on a mass scale M that decreases exponentially as the lattice spacing a goes to zero. On the other hand, Gross [8] has proven that in the "naive" continuum limit where the coupling and energy scale is held fixed as a goes to zero, that the Villain version of the model, at least, does indeed converge to free electromagnetic theory at the level of $F_{\mu\nu}$ or the Wilson loops, as of course it was designed to do. On this basis it was predicted in I that the finite-size scaling behaviour following from the effective Lagrangian theory should be valid not for arbitrarily large lattice size, but for intermediate lattice sizes L obeying

$$1 \ll L \ll 1/Ma \tag{1.1}$$

where M is the mass scale referred to above. One of the objectives of the present work is to test these predictions against numerical data.

---

[1]Although their argument was actually for the noncompact theory in (2+1) D.

The U(1) model in (2+1) dimensions has been well explored, by approaches including variational approximations [9-17], strong-coupling series expansions [18-23], the related t-expansion [24,25], a finite-lattice approach [26], block renormalization group [27], momentum-space lattice [28] and quantum Monte Carlo simulations [29-36]. It is perhaps the one lattice gauge model where the bulk behaviour is more precisely known in the Hamiltonian that in the Euclidean formulation. None of the previous finite-lattice or Monte Carlo calculations, however, have been of sufficient accuracy to give a reliable picture of the finite-size scaling behaviour.

It is probably fair to say that the development of Hamiltonian Monte Carlo methods in lattice gauge theory lags behind Euclidean methods by about a decade. The approaches used hitherto [29-36] have usually used a strong-coupling (electric field) representation, giving rise to a discrete set of basis states. Unfortunately, an attempt to apply a similar technique to the non-Abelian $SU(2)$ gauge theory failed, because it appeared to run into the infamous "minus sign" problem. There is a need, therefore, to develop methods based on a weak-coupling representation, which should be able to avoid this problem, for a pure gauge theory at least. That is the second objective of the present work.

A weak-coupling algorithm was in fact developed by Heys and Stump [29], and Chin, Negele and Koonin [37], based on the Green's Function Monte Carlo techniques of Kalos and collaborators [38]. In later work, however, Chin etal. preferred to use the Monte Carlo technique as a tool in variational approximations. This introduces an unknown systematic bias due to the form of the variational wave function, which can be quite serious, especially for local observables such as mass gaps. Here we prefer an "unbiased" form of the original algorithm [38], in which a trial wave-function is indeed used to guide the random walkers in the ensemble towards the most likely region of configuration space [39], but the results should be independent of this guidance.

In Section II of the paper, we summarize the predictions from effective Lagrangian theory and weak-coupling perturbation theory obtained in reference I. In Section III we discuss the Monte Carlo method, and in Section IV the results are presented. Our conclusions are set out in Section V.

II. THEORETICAL PREDICTIONS

A. Effective Lagrangian Theory

An effective Lagrangian approach to the compact U(1) lattice gauge theory was discussed in reference I. The leading term in the Euclidean effective action was taken to be that of a free photon field:

$$S = \frac{\rho}{4} \int d^{D+1}x F_{\mu\nu} F_{\mu\nu} \tag{2.1}$$

where

$$F_{\mu\nu} = \partial_\mu A_\nu - \partial_\nu A_\mu \tag{2.2}$$

The coupling parameter ρ we shall refer to as the "helicity modulus", by analogy with spin-wave theory, for lack of a better name. The interactions between the photons are "soft" at

low energies [5,I], and equation (2.1) is sufficient to predict the leading terms in a systematic large-volume expansion of the theory.

Starting from this point, it was shown in I that the finite-size corrections to the ground-state energy per site for the $(D+1)$ dimensional model should have a universal form:

$$\epsilon_o(L) - \epsilon_o(\infty) \underset{L\to\infty}{\sim} -\frac{(D-1)v}{2L^{D+1}}[\alpha^{(D)}_{-1/2}(1) + 2 - \frac{2}{D+1}] \quad , \tag{2.3}$$

corresponding to the Casimir energy of $(D-1)$ massless boson degrees of freedom, where $\alpha^{(D)}_{-1/2}(1)$ is a known "shape coefficient"[2], v is the speed of light in the theory, and L is the number of sites on an edge of the lattice (assuming periodic boundary conditions). For $D=2$, this reduces to

$$\epsilon_o(L) - \epsilon_o(\infty) \underset{L\to\infty}{\sim} -\frac{0.7188v}{L^3} \tag{2.4}$$

The finite-size behaviour of the axial string tension on the lattice was also predicted:

$$\sigma \underset{L\to\infty}{\sim} \frac{v^2}{2\rho L^{D-1}} \tag{2.5}$$

or for $D=2$,

$$\sigma \underset{L\to\infty}{\sim} \frac{v^2}{2\rho L} \tag{2.6}$$

Now it is known [40,7] that the compact U(1) lattice model in (2+1) dimensions is not in fact a massless theory, but a confining one, with boson excitations of mass M estimated by Gopfert and Mack [7] to behave as

$$Ma \underset{a\to 0}{\sim} \frac{c_1}{g^2}\exp(-\frac{c_2}{g^2}) \tag{2.7}$$

where c_1 and c_2 are constants, and $g^2 = e^2 a$, with e being the bare lattice electric charge and a the lattice spacing. It was therefore argued in I that the predictions (2.4) and (2.6) should be valid not for arbitrarily large lattice sizes L, but only for intermediate distance scales

$$1 \ll L \ll 1/Ma \quad , \tag{2.8}$$

remaining less than the Compton wavelength of the massive bosons.

B. Weak-coupling Perturbation Theory

Weak-coupling perturbation expansions for the lattice model have also been discussed in reference I. The quantum Hamiltonian for the model can be written as [9,41]

$$H = \sum_l E_l^2 - 2x\sum_P cos\Theta_P \tag{2.9}$$

where l denotes links and P denotes plaquettes of the 2-dimensional spatial lattice. Here E_l is the "electric field" on link l, and the plaquette angle Θ_P can be written in the usual way as

$$\Theta_P = A_1 + A_2 - A_3 - A_4 \tag{2.10}$$

in terms of gauge fields A_k on links $k = 1, 2, 3, 4$ surrounding the plaquette. The electric field E_l and gauge field A_k are conjugate variables:

$$[E_l, A_k] = -i\delta_{lk} \tag{2.11}$$

The strong-coupling parameter $x = 1/e^4a^2 = 1/g^4$.

By Taylor expanding the cosine in equation (2.9), Fourier transforming, and performing a Bogoliubov transformation, one obtains an equivalent boson (i.e. photon) Hamiltonian with one independent degree of freedom per site. Terms up to second order in the fields are diagonalized by the Bogoliubov transformation, and higher order terms can be treated as perturbations, leading to an expansion in powers of $x^{-1/2}$. Using Rayleigh-Schrödinger perturbation theory, the following results were obtained. The ground-state energy per site was found to be:

$$\begin{aligned}\epsilon_o(L) &= \frac{E_o}{L^2} \\ &= -2x + 1.916183x^{1/2} - 0.2294848 - 0.0268602x^{-1/2} - 0.009315x^{-1} + O(x^{-3/2}) \\ &\quad - \frac{1}{L^3}[1.4376x^{1/2} - 0.34434 - 0.07533x^{-1/2} - 0.0421x^{-1} + O(x^{-3/2})]\end{aligned} \tag{2.12}$$

The energy $E(\vec{k})$ of a single photon state with momentum $\vec{k}$ was calculated, and from the dispersion relation

$$E(\vec{k}) \underset{k\to 0}{\sim} v\vec{k} \tag{2.13}$$

the speed of light was computed as

$$v = 2x^{1/2} - 0.479046 - 0.104783x^{-1/2} - 0.05847x^{-1} + O(x^{-3/2}) \tag{2.14}$$

Finally, the axial string tension in the model can be computed. It is dominated by the "zero modes" at weak coupling, and is given by

$$\sigma = 1/L \tag{2.15}$$

exact to all orders in the weak-coupling expansion (but not accounting, of course, for non-perturbative effects.).

The results (2.12) and (2.14) agree precisely, to the order calculated, with the effective Lagrangian prediction (2.4). The result (2.15) also agrees with (2.6), provided that

$$\frac{v^2}{2\rho} = 1 \tag{2.16}$$

which then is an identity relating the parameters of the effective Lagrangian for this particular lattice system.

III. MONTE CARLO METHODS

We have carried out one set of finite-lattice calculations using a strong-coupling set of basis states, namely eigenstates of the electric field operator E_l on each link. Since the gauge field variable A_k is taken to lie in the compact domain $[0, 2\pi]$, the conjugate electric field is quantized, $E_l = 0, \pm 1, \pm 2, \ldots$, so that the strong-coupling basis is discrete. We employed the method of "stochastic truncation" used previously in a study of the (3+1) D model by Hamer and Aydin [42], which needs no further discussion here.

We also wished to develop and test a technique suitable for use with a weak-coupling representation. The weak-coupling states are taken to be eigenstates of the plaquette angles Θ_P, which can take continuous values, and previous methods [29-36] are inappropriate to such a case. Instead, we have chosen to use the Green's Function Monte Carlo [GFMC] method [38,39], a version of which was discussed by Heys and Stump [29], and Chin et al [37]. A brief summary of the method can be given as follows.

A. Ground-state Energy

In a weak-coupling representation, the Hamiltonian (2.9) can be written symbolically as:

$$H = -\sum_l \frac{\partial^2}{\partial A_l^2} + V(\Theta) \tag{3.1}$$

where

$$V(\Theta) = -2x \sum_P \cos \Theta_P \tag{3.2}$$

and the plaquette angles Θ_P and link angles A_l are related by (2.10). The imaginary time Schrodinger equation for the system is

$$-\frac{\partial}{\partial t}\Phi(\Theta, t) = \left[-\sum_l \frac{\partial^2}{\partial A_l^2} + V(\Theta) - E_T\right] \Phi(\Theta, t) \tag{3.3}$$

where E_T is a trial energy, representing a constant shift in the zero of energy, which will prove useful. At large times t the component corresponding to the ground-state will dominate

$$\Phi(\Theta, t) \tilde{\iota}_{\sim\infty} c_o \exp[-(E_o - E_T)t]\Phi_o(\Theta) \tag{3.4}$$

where $\Phi_o(\Theta)$ is the ground-state eigenfunction, provided the initial state is not orthogonal to Φ_o.

Equation (3.3) is a diffusion equation in configuration space, and is easily simulated by the Green's Function Monte Carlo method. It is assumed that the ground-state wave function can be chosen positive everywhere, and it is simulated by the density distribution of an ensemble of random walkers in configuration space. The first term on the right of equation (3.3) produces diffusion, and is simulated by a Gaussian random walk of the members of the ensemble as time proceeds, while the term $[V(\Theta) - E_T]$ produces a growth or decay in the density which is simulated by a branching process.

The efficiency of the simulation is greatly increased by the use of variational guidance or importance sampling [39]. Let $\Psi_T(\Theta)$ be a variational approximation to the true ground-state wave function, and define a new probability distribution

$$f(\Theta, t) = \Phi(\Theta, t)\Psi_T(\Theta) \tag{3.5}$$

Then the modified imaginary time Schrodinger equation for f reads:

$$-\frac{\partial f}{\partial t} = -\sum_l \frac{\partial^2 f}{\partial A_l^2} + (E_L(\Theta) - E_T)f + \sum_l \frac{\partial}{\partial A_l}(f F_{Ql}(\Theta)) \tag{3.6}$$

Here

$$E_L(\Theta) = \frac{1}{\Psi_T} H \Psi_T \tag{3.7}$$

is the local energy obtained from the trial function, and

$$F_{Ql}(\Theta) = \frac{2}{\Psi_T}\frac{\partial \Psi_T}{\partial A_l} \tag{3.8}$$

is a "quantum force" term, which turns out to produce a directed drift in the ensemble. By a good choice of Ψ_T and E_T the "excess local energy" term $(E_L(\Theta) - E_T)$ can be made very small, which reduces the amount of branching necessary, and reduces fluctuations in the results.

For small time steps Δt, an approximate Green's function solution to equation (3.6) is

$$\begin{aligned} G(\Theta - \Theta', \Delta t) \simeq & \exp[-(E_L(\Theta) - E_T)\Delta t] \\ & \times \prod_l \{\frac{1}{\sqrt{4\pi\Delta t}} \exp[-(A_l' - A_l - \Delta t F_{Ql}(\Theta))^2/4\Delta t]\} \end{aligned} \tag{3.9}$$

In the Monte Carlo simulation, each iteration corresponds to a time step Δt. At each iteration, we sweep through each link in turn, and simulate the corresponding exponential factor in the curly bracket in (3.9) by a random displacement of the link variable for each walker

$$\Delta A_l = \Delta t F_{Ql}(\Theta) + \chi \tag{3.10}$$

where χ is randomly chosen from a Gaussian distribution with standard deviation $\sqrt{2\Delta t}$. The first term in (3.10) is the "drift" term, and the second is the "diffusion" term. The first exponential on the right of (3.9) is simulated by multiplying the "weight" of each walker by an equivalent amount.

At the end of each iteration, the trial energy E_T is adjusted to compensate for any change in the total weight of all walkers in the ensemble; and a "branching" process is carried out, so that walkers with weight greater than (say) 2 are split into two new walkers, while any two walkers with weight less than (say) 1/2 are combined into one, chosen randomly according to weight from the originals. This procedure of "Runge smoothing" [42] maximizes statistical accuracy by keeping the weights of all the walkers within fixed bounds, while minimizing any fluctuations in the total weight due to the branching process.

When equilibrium is reached after many sweeps through the lattice, the average value of the trial energy E_T will give an estimate of the ground-state energy E_o; and the weight density of the ensemble in configuration space will be proportional to $\Phi_o \Psi_T$. Various corrections due to the finite time interval Δt have been ignored in this discussion, and the limit $\Delta t \to 0$ must be taken in some fashion to eliminate such corrections.

In the simulations presented here, the trial function for the ground state was chosen as [37]

$$\Psi_T(\Theta) = \exp[c \sum_P \cos \Theta_P] \tag{3.11}$$

where the constant c is a variational parameter to be optimized. Then the local trial energy is

$$E_L(\Theta) = \Psi_T^{-1}[-\sum_l \frac{\partial^2}{\partial A_l^2} - 2x \sum_P \cos \Theta_P]\Psi_T \tag{3.12}$$

$$= -2x \sum_P \cos \Theta_P - \sum_l [c^2(\sin \Theta_{p2,l} - \sin \Theta_{p1,l})^2 - c(\cos \Theta_{p1,l} + \cos \Theta_{p2,l})] \tag{3.13}$$

and the quantum force term is

$$F_{Ql}(\Theta) = 2c(\sin \Theta_{p2,l} - \sin \Theta_{p1,l}) \tag{3.14}$$

The configuration variables are taken to be the plaquette angles, and in equations (3.13) and (3.14) the symbols $p1$, $p2$ denote the two plaquettes adjacent to the link l, such that a change ΔA_l in the link angle produces changes

$$\Delta \Theta_{p1,l} = \Delta A_l \quad , \quad \Delta \Theta_{p2,l} = -\Delta A_l \tag{3.15}$$

in the plaquette angles.

B. The Mean Plaquette

An observable we would like to measure is the ground-state expectation value of the plaquette operator

$$P = \langle \cos \Theta_P \rangle_0 \tag{3.16}$$

By the Feynman-Hellmann theorem, this is related to the slope of the ground-state energy per site

$$P = -\frac{1}{2L^2} \frac{dE_0}{dx} \tag{3.17}$$

In the strong-coupling, stochastic truncation algorithm, this derivative can be estimated using the technique discussed by Price et al [43]. A similar technique involving "secondary amplitudes" also works for the GFMC algorithm, as follows. Consider a small increment Δ in the coupling x: then we can write the Hamiltonian as

$$H = H_o(x) + \Delta H_1 \tag{3.18}$$

where $H_o(x)$ is the Hamiltonian (3.1), and

$$H_1 = -2 \sum_P \cos \Theta_P \tag{3.19}$$

Perform a Taylor expansion for the eigenvector and eigenvalue:

$$|f(x+\Delta,t\rangle = |f_o(x,t)\rangle + \Delta |f_1(x,t)\rangle + O(\Delta^2) \tag{3.20}$$

$$E_o(x+\Delta) = E_o(x) + \Delta E_o'(x) + O(\Delta^2) \tag{3.21}$$

and substitute in the evolution equation (ignoring any variational guidance for the time being):

$$|f(x+\Delta, t+\Delta t)\rangle = e^{-(H-E_o(x+\Delta))\Delta t} |f(x+\Delta,t)\rangle \tag{3.22}$$

where the exact ground state energy is here being used for the trial energy. Now expand equation (3.22), and equate powers of Δ, to obtain

$$|f_o(x,t+\Delta t)\rangle = e^{-(H-E_o(x))\Delta t} |f_o(x,t)\rangle \tag{3.23}$$

and

$$|f_1(x,t+\Delta t)\rangle = e^{-(H-E_o(x))\Delta t} |f_1(x,t)\rangle + \Delta t (E_o'(x) - H_1) |f_o(x,t)\rangle \tag{3.24}$$

The Monte Carlo algorithm is now straightforward, based on equations (3.23) and (3.24). Each walker in the ensemble now carries a "primary" weight f_o and a "secondary" weight f_1, and trial values E_T and E_T' are chosen to approximate E_o and E_o'. At each iteration the primary weight f_o evolves exactly as before, while the weight f_1 is treated similarly, except for the addition of a second term on the right of (3.24), proportional to f_o. At the end of each iteration, E_T is adjusted to compensate for any change in the sum of the weights f_o, while E_T' is adjusted to compensate for any change in the sum of the weights f_1. At equilibrium, the average value of E_T estimates E_o, and the average of E_T' estimates E_o'. The addition of variational guidance only modifies the simulation of the first, exponential terms in (3.23) and (3.24), in the way discussed above.

A similar technique could be used for the expectation value of any operator which is diagonal in the weak-coupling representation.

C. Mass Gaps

The calculation of mass gaps in an unbiased fashion is a difficult task. One option in the weak-coupling representation would be to adopt the standard Euclidean Monte Carlo techniques, and analyze correlation functions on the spatial lattice as functions of distance. A drawback with this approach in the Hamiltonian formulation is that one needs to know the "speed of light" in order to translate a spatial correlation length into an energy gap. Dimensionless mass ratios could be directly predicted, however, and although we have not attempted it here, the method deserves exploration in future work.

We have chosen to try two different techniques, one for the "antisymmetric" glueball state, and the other for the "symmetric" glueball state.

The antisymmetric glueball state lies in a different symmetry sector from the vacuum state, and in the strong-coupling limit it can be formed by acting on the vacuum with the operator $S = \sum_P sin\Theta_P$. The weak-coupling wavefunction should therefore be anti-symmetric in the variable S, and we can employ the "fixed node" method of Reynolds et al. [44]. The wave-function is assumed anti-symmetric in S, and chosen positive for $S \geq 0$; the simulation is then carried out only for values $S > 0$. The ensemble evolves exactly as before, except that when a walker crosses the boundary $S = 0$ it is assumed to "annihilate" with a "mirror-image" walker carrying negative weight coming from the other side, and is removed from the ensemble. Subtracting the vacuum energy from the energy found for this antisymmetric state, we **should** obtain a measure of the antisymmetric glueball mass. Unfortunately, our attempts to apply this technique have been unsuccessful so far.

The "symmetric" glueball state lies in the same sector as the vacuum state, and in the strong-coupling limit it can be formed by acting on the vacuum with the operator $C = \sum_P \cos\Theta_P$. To measure its mass, we adopted the simple strategy of "exciting" the vacuum periodically during the simulation, and then measuring the rate at which the trial energy or "score" decays back to its equilibrium value as a function of Euclidean time. The excitation process involved multiplying the absolute value of the weight of each walker by a factor proportional to $[\sum_P \cos\Theta_P - NP]$, where P is the mean plaquette value, which should produce a state approximately orthogonal to the ground state. Both positive and negative weights now occur, and are evolved separately according to the same rules as before.

IV. RESULTS

The stochastic truncation method, and strong-coupling basis, were used to calculate the ground-state energy per site, the mean plaquette value, and the string tension in the model for lattices up to 10×10 sites. The algorithm was much the same as used previously [6] for the (3+1) D model, except that "Runge smoothing" [42] was added in the branching process to reduce fluctuations. Production runs for each lattice size and coupling value consisted of 20K iterations or sweeps, with an ensemble size of 10K configurations. The first 2K iterations were discarded to allow for equilibration, and the results were averaged over blocks of 640 iterations before estimating the error to minimize correlation effects.

The GFMC method, and weak-coupling basis, were also used to calculate the ground-state energy and mean plaquette, as well as the mass gaps, using the algorithms described in the previous section. At each coupling, the variational parameter c was adjusted to minimize the error by a series of trial runs. The ensemble size for a production run was typically 5K, and the number of iterations varied from 20K up to 120K. The results are outlined in what follows.

A. Ground-State Energy

For the GFMC method, our first task is to analyze the dependence on the time interval Δt. Figure 1 shows estimates of the ground-state energy for lattice size $L = 4$ at a coupling

$x = 1$, obtained using various values of Δt, and two different values of the variational parameter c. The data can be well fitted by a linear dependence on Δt. It can be seen that the results depend strongly on c at $\Delta t = 0.1$, but when the straight lines are extrapolated to $\Delta t = 0$ the results for both values of c agree with each other, and with the strong-coupling result, within errors. In subsequent work, estimates were made at $\Delta t = 0.05$ and $\Delta t = 0.005$ and extrapolated to $\Delta t = 0$ assuming a linear dependence on Δt. It may be worth noting that the optimum value of c at $x = 1$ is $c \approx 0.42$, and at that value the dependence on Δt has almost disappeared.

The final weak-coupling estimates can now be compared with those obtained from the strong-coupling algorithm. They are found to be reasonably consistent: their error bars overlap in 60 % of cases, and their accuracy is also quite comparable. This provides evidence that both algorithms are working correctly. A table of estimates of the ground-state energy per site is given in Table I.

The finite-size dependence of these results is illustrated in Figure 2. At strong couplings (small x), the finite lattice results converge exponentially fast to their bulk limit, as can be seen from a glance at Table I. At weak couplings or large x values, as in Figure 2b, the finite-size results are well fitted by a straight line in $1/L^3$, as predicted by equations (2.4) and (2.12), unless L becomes too large, when the curve levels off. A hint of this is seen for $L = 10$ in Figure 2b, and it happens for $L \geq 5$ in Figure 2a. The straight line in Figure 2b corresponds to

$$\epsilon_o(L) = -4.414 - \frac{2.60}{L^3} \tag{4.1}$$

whereas the series result (2.12) at $x = 4$ gives

$$\epsilon_o(L) = -4.413(2) - \frac{2.48(1)}{L^3} \tag{4.2}$$

The agreement is remarkable.

Extrapolating these curves to $L \to \infty$, one obtains estimates of the bulk limit which are listed in Table I, and graphed in Figure 3. Also shown for comparison are strong-coupling series estimates [23], and some results from the t-expansion of Morningstar [25]. The overall agreement between the results is excellent. At strong coupling the series estimates are of course the most accurate, but by $x = 4$ the Monte Carlo results are better.

B. Mean Plaquette Value

The weak-coupling algorithm for estimating P was discussed in Section III. When extrapolated to $\Delta t = 0$, the results are found once again to agree quite well with those from the strong-coupling algorithm. A table of results is given in Table II. The finite-size scaling behaviour follows from that of the ground-state energy, by equation (3.17), and will not be discussed further. Extrapolating to $L \to \infty$, estimates of the bulk limit are obtained, which are listed in Table II, and graphed in Figure 4. The agreement with series [23] and t-expansion [25] results is once again excellent. The variation of P with coupling x is extremely smooth, with no sign of any phase transition, as we should expect [7].

C. String Tension

In the strong-coupling representation, the axial string tension can be calculated as usual [6] via the formula

$$\sigma = \frac{1}{L}(E_s - E_o) \tag{4.3}$$

where E_s is the energy of the lowest state in the string sector, with a string of unit electric flux wrapping around the periodic lattice. In the weak-coupling representation the calculation is more difficult, because the basis states are no longer eigenstates of the electric flux. Since the strong-coupling results are quite satisfactory, we have restricted our attention to them.

Results for the string tension are listed in Table III, and graphed in Figure 5. The first obvious feature is that at large x the finite-lattice results very rapidly level off at the value $\sigma(L) = 1/L$ predicted by equation (2.15). At a given coupling, this behaviour will hold until L becomes so large that $\sigma(L)$ becomes comparable with the exponentially small bulk string tension. The prediction of reference I is thus verified. At $x = 4$, equation (2.15) describes the data right up to $L = 10$.

Estimates of the bulk limit are also presented in Table III, along with[2] some values obtained by Irving and Hamer [21] using an "exact linked cluster expansion" (ELCE). The convergence of the finite-lattice values to the bulk limit is not as rapid as for the ground-state energy, and so the accuracy of the extrapolation to $L \to \infty$ is not nearly so good. Nevertheless, the agreement with the ELCE estimates seems reasonably satisfactory, apart from a small discrepancy at $x = 1$.

D. Mass Gaps

As outlined in section III c, the mass of the "symmetric" glueball state can be estimated by "exciting" the ground-state ensemble periodically, and measuring the rate of relaxation back to the ground-state. An example of the results is shown in Figure 6. Here the system has been excited every 400 iterations, and the results have been averaged over many repetitions of the process. It can be seen that the data for the "score" (or trial energy) are well fitted by an exponential decay curve

$$S(t) = S_o + ae^{-mt} \tag{4.4}$$

and it can be checked that the asymptotic value S_o agrees with the ground-state equilibrium score or energy. The parameters of the fit carry a statistical error, of course, and depend quite strongly on the range over which the fit is made, so that the resulting estimate of the mass m was found to be accurate to only about 10 %. At this level, the estimates were in approximate agreement with earlier finite-lattice [26] and series [23] works, but it is hardly worthwhile to present any more quantitative results.

---

[2]Strong coupling series expansions cannot be used here because of the problem of "roughening".

V. CONCLUSIONS

The first aim of this project was to study the finite-size scaling behaviour of the model. The data have confirmed very nicely that the predictions of effective Lagrangian theory and weak-coupling perturbation theory [4] are indeed correct, provided that one remains at intermediate distance scales

$$1 \ll L \ll 1/Ma \tag{5.1}$$

where the mass scale M is given by equation (2.7).

The interpretation of this fact may be open to more debate. It appears that at scales given by equation (5.1) the theory behaves like a theory of free, massless photons. This fits with the conclusion of Gross [8], who showed formally that the model does converge to free electromagnetic theory in the naive continuum limit $a \to 0$ with e^2 fixed. If, on the other hand, one renormalizes the coupling in the usual way so that M remains fixed as $a \to 0$, then on this smaller energy scale, or larger distance scale, one obtains the confining theory of free massive bosons discussed by Göpfert and Mack [7]. There is no inherent conflict between these statements, because the ratio between the two energy scales becomes infinite in the limit $a \to 0$. Thus it would appear that the same lattice model can give rise to two different continuum theories, depending on the way in which the continuum limit is taken.

Our second aim was to implement and test an unbiased quantum Monte Carlo method based on a weak-coupling representation for this gauge model. We have chosen to use the Green's Function Monte Carlo method [37-39]. It was found to work extremely well for the ground-state energy and its first derivative (the mean plaquette), being accurate to about 0.01 % for the energy and 0.5 % for the mean plaquette at a coupling $x = 2$ in the scaling region, and agreeing within errors with strong-coupling series estimates. Thus the viability of the method is established.

The string tension was measured using a strong-coupling basis rather than the weak-coupling one; but there seems no reason why Wilson loops and Creutz ratios should not be measured by similar techniques to those used for the mean plaquette. This would give the tension as an inverse area: translation to an energy per unit length would require knowledge of the speed of light.

Attempts were also made to measure mass gaps using two different methods. For the antisymmetric glueball state, a "fixed node" technique was tried, but it failed for reasons which are still not understood. For the symmetric glueball state, we simply measured the exponential decay in Euclidean simulation time of an excited state system. This technique gave reasonably convincing results, but only at a level of 10 % or so in accuracy. This is not really satisfactory for quantitative work, and more sophisticated procedures will need to be considered in the future.

ACKNOWLEDGMENTS

We are very grateful to the Supercomputer Facility of the Australian National University for a grant of time on their Fujitsu VP2200 Supercomputer. We would also like to thank Dr. Russell Standish and the Special Research Centre for Parallel Computing at the University of NSW for the use of their CM5 machine. Finally, we are grateful for the help and advice given by Dr. Zheng Weihong during the course of this work.

REFERENCES

1. J. Gasser and H. Leutwyler, Nucl. Phys. **B307**, 763 (1988)
2. P. Hasenfratz and H. Leutwyler, Nucl. Phys. **B343**, 241 (1990)
3. P. Hasenfratz and F. Niedermayer, Bern Report No. BUTP-92/46 (unpublished)
4. C. J. Hamer and Zheng Weihong, Phys. Rev. **D48**, 4435 (1993)
5. A. Kovner, B. Rosenstein and D. Eliezer, Nucl. Phys. **B350**, 325 (1991)
6. C. J. Hamer and M. Aydin, Phys. Rev. **D43**, 4080 (1991)
7. M. Göpfert and G. Mack, Commun. Math. Phys. **82**, 545 (1982)
8. L. Gross, Commun. Math. Phys. **92**, 137 (1983)
9. S. D. Drell, H. R. Quinn, B. Svetitsky and M. Weinstein, Phys. Rev. **D19**, 619 (1979)
10. D. Horn and M. Weinstein, Phys. Rev. **D25**, 3331 (1982)
11. U. Heller, Phys. Rev. **D23**, 2357 (1981)
12. P. Suranyi, Phys. Letts. **122B**, 279 (1983); Nucl. Phys. **B225**, 77 (1983)
13. H. Arisue, M. Kato and T. Fujiwara, Prog. Theor. Phys. **70**, 229 (1983)
14. W. Langguth, Z. Phys. **C23**, 289 (1986)
15. D. W. Heys and D. R. Stump, Nucl. Phys. **B257**, 19 (1985); **ibid B285**, 13 (1987)
16. Guo Shuohong, Zheng Weihong and Liu Jiunming, Phys. Rev. **D38**, 2591 (1988)
17. A. Dabringhaus, M. L. Ristig and J. W. Clark, Phys. Rev. **D43**, 1978 (1991)
18. J. Kogut, D. K. Sinclair and L. Susskind, Nucl. Phys. **B114**, 199 (1976)
19. V. Alessandrini, V. Hakim and A. Krzywicki, Nucl. Phys. **B200**, 355 (1982)
20. A. C. Irving and C. J. Hamer, Nucl. Phys. **B230**, 361 (1984)
21. A. C. Irving and C. J. Hamer, Nucl. Phys. **B235**, 358 (1984)
22. C. J. Hamer and A. C. Irving, Z. Phys. **C27**, 145 (1985)
23. C. J. Hamer, J. Oitmaa and Zheng Weihong, Phys. Rev. **D45**, 4652 (1992)
24. D. Horn, G. Lana and D. Schreiber, Phys. Rev. **D36**, 3218 (1987)
25. C. J. Morningstar, Phys. Rev. **D46**, 824 (1992)
26. A. C. Irving, J. F. Owens and C. J. Hamer, Phys. Rev. **D28**, 2059 (1983)

27. G. Lana, Phys. Rev. **D38**, 1954 (1988)

28. A. M. Chaara, H. Kröger, K. J. M. Moriarty and J. Potvin, Universite-Laval preprint 1992

29. D. W. Heys and D. R. Stump, Phys. Rev. **D28**, 2067 (1983)

30. J. Potvin and T. A. DeGrand, Phys. Rev. **D30**, 1285 (1984)

31. T. A. DeGrand and J. Potvin, Phys. Rev. **D31**, 871 (1985)

32. D. Dahl and R. Blankenbecler, Phys. Rev. **D32**. 977 (1985)

33. S. E. Koonin, E. A. Umland and M. R. Zirnbauer, Phys. Rev. **D33**, 1795 (1986)

34. S. M. Eleuterio and R. V. Mendes, J. Phys. **A20**, 6411 (1987)

35. C. M. Yung, C. R. Allton and C. J. Hamer, Phys. Rev. **D39**, 3778 (1989)

36. D. Kotchan, Ph.D. thesis, Toronto 1990 (referred to in ref. 25)

37. S. A. Chin, J. W. Negele and S. E. Koonin, Ann. Phys. (N.Y.) **157**, 140 (1984)

38. D. M. Ceperley and M. H. Kalos, in "Monte Carlo Methods in Statistical Mechanics", ed. K. Binder (Springer-Verlag, New York, 1979), p. 145

39. M. H. Kalos, D. Levesque and L. Verlet, Phys. Rev. **A9**, 2178 (1974)

40. A. M. Polyakov, Nucl. Phys. **B120**, 429 (1977)

41. J. Kogut and L. Susskind, Phys. Rev. **D11**, 395 (1975)

42. K. J. Runge, Lawrence Livermore preprint 1991

43. P. F. Price, C. J. Hamer and D. O'Shaughnessy, J. Phys. **A26**, 2855 (1993)

44. P. J. Reynolds, D. M. Ceperley, B. J. Alder and W. A. Lester, J. Chem. Phys. **77**, 5593 (1982)

FIGURE CAPTIONS

Fig.1 Dependence on time interval Δt of estimates of the ground-state energy obtained via the weak-coupling algorithm for a lattice size $L = 4$ at coupling $x = 1$. Results are shown for two different values of the variational parameter c. The point at $\Delta t = 0$ was obtained via the strong-coupling algorithm.

Fig.2 Finite-size dependence of estimates of the ground-state energy per site: a) at coupling $x = 2$; b) at $x = 4$. The curve in a) is merely to guide the eye; the curve in b) is a straight line.

Fig.3 The ground-state energy per site ϵ_o as a function of coupling x in the bulk limit. The points are Monte Carlo estimates, and the line graphs estimates from a strong-coupling series analysis [23].

Fig.4 The mean plaquette P as a function of coupling x in the bulk limit. The points are Monte Carlo estimates, and the solid line shows results from a strong-coupling series analysis.

Fig.5 The string tension σ as a function of coupling x and lattice size L. The points are Monte Carlo results for various lattice sizes; the solid line shows estimates of the bulk limit from an ELCE technique [2].

Fig.6 The "score", or trial energy (in arbitrary units), at coupling $x = 2$, lattice size $L = 3$, and time interval $\Delta t = 0.005$, as a function of the number of iterations following an excitation. The solid line is a least-squares fit of the form (4.4).

TABLE I

Values for the ground-state energy per site $\epsilon_o(L)$ as a function of lattice size L and coupling x. Also listed are extrapolated estimates of the bulk limit $L \to \infty$, together with strong-coupling series estimates [23] and some t-expansion results [25].

L	x = 0.5	1.0	1.5	2.0	4.0
2	0.1318(1)	0.5386(2)	1.1200(5)	1.7880(2)	4.7786(2)
3	0.12273(4)	0.4691(1)	0.9897(2)	1.6172(1)	4.5138(1)
4	0.12266(2)	0.4651(2)	0.9701(2)	1.5824(2)	4.4543(2)
5	0.12266(2)	0.4651(2)	0.9677(2)	1.5729(2)	4.4342(2)
6		0.4652(1)	0.9673(2)	1.5708(3)	4.4254(2)
8		0.4652(2)	0.9670(4)	1.5700(2)	4.4186(4)
10	0.12265(1)	0.4649(2)	0.9675(3)	1.5699(3)	4.4172(3)
$L \to \infty$	0.12265(1)	0.4651(2)	0.9673(4)	1.5699(3)	4.414(2)
Series	0.1226698	0.46509	0.96729	1.5700(1)	4.43(2)
t-expansions		0.465(1)			4.408(2)

TABLE II

Mean plaquette values P as a function of coupling x and lattice size L. Also listed are the resulting estimates of the bulk limit $L \to \infty$, and estimates obtained from a strong-coupling series expansion [23] and t-expansion [25].

L	x = 0.5	1.0	1.5	2.0	4.0
2	0.279(2)	0.5177(6)	0.6325(9)	0.6909(4)	0.7854(3)
3	0.2431(7)	0.4425(4)	0.5856(7)	0.6585(3)	0.7661(2)
4	0.2446(8)	0.4342(5)	0.5656(8)	0.6487(6)	0.7620(3)
5	0.2453(8)	0.4335(3)	0.5605(7)	0.641(2)	0.7594(2)
10	0.2408(2)	0.432(2)	0.558(2)	0.638(2)	0.7558(8)
$L \to \infty$	0.241(1)	0.433(1)	0.558(2)	0.639(3)	0.756(1)
Series	0.240775	0.43336	0.56083(4)	0.6382(5)	0.80(3)
t-expansion		0.4333(3)			0.757(4)

TABLE III

Values for the string tension σ as a function of coupling x and lattice size L. Also listed are estimates of the bulk limit $L \to \infty$, and some estimates derived from an ELCE technique [21].

L	x = 0.5	1.0	1.5	2.0	4.0
2	0.7809(2)	0.5844(5)	0.520(1)	0.5077(5)	0.4998(7)
3	0.8438(5)	0.5520(6)	0.397(1)	0.3519(6)	0.335(1)
4	0.8716(4)	0.573(1)	0.367(1)	0.284(1)	0.250(2)
5	0.8838(4)	0.590(1)	0.369(1)	0.255(1)	0.200(2)
6		0.601(1)	0.377(2)	0.246(2)	0.166(2)
8		0.610(2)	0.383(3)	0.246(2)	0.121(4)
10	0.8981(1)	0.612(4)	0.396(5)	0.251(5)	0.103(5)
$L \to \infty$	0.900(2)	0.614(5)	0.39(1)	0.28(1)	
ELCE	0.902(1)	0.601(1)		0.282(2)	

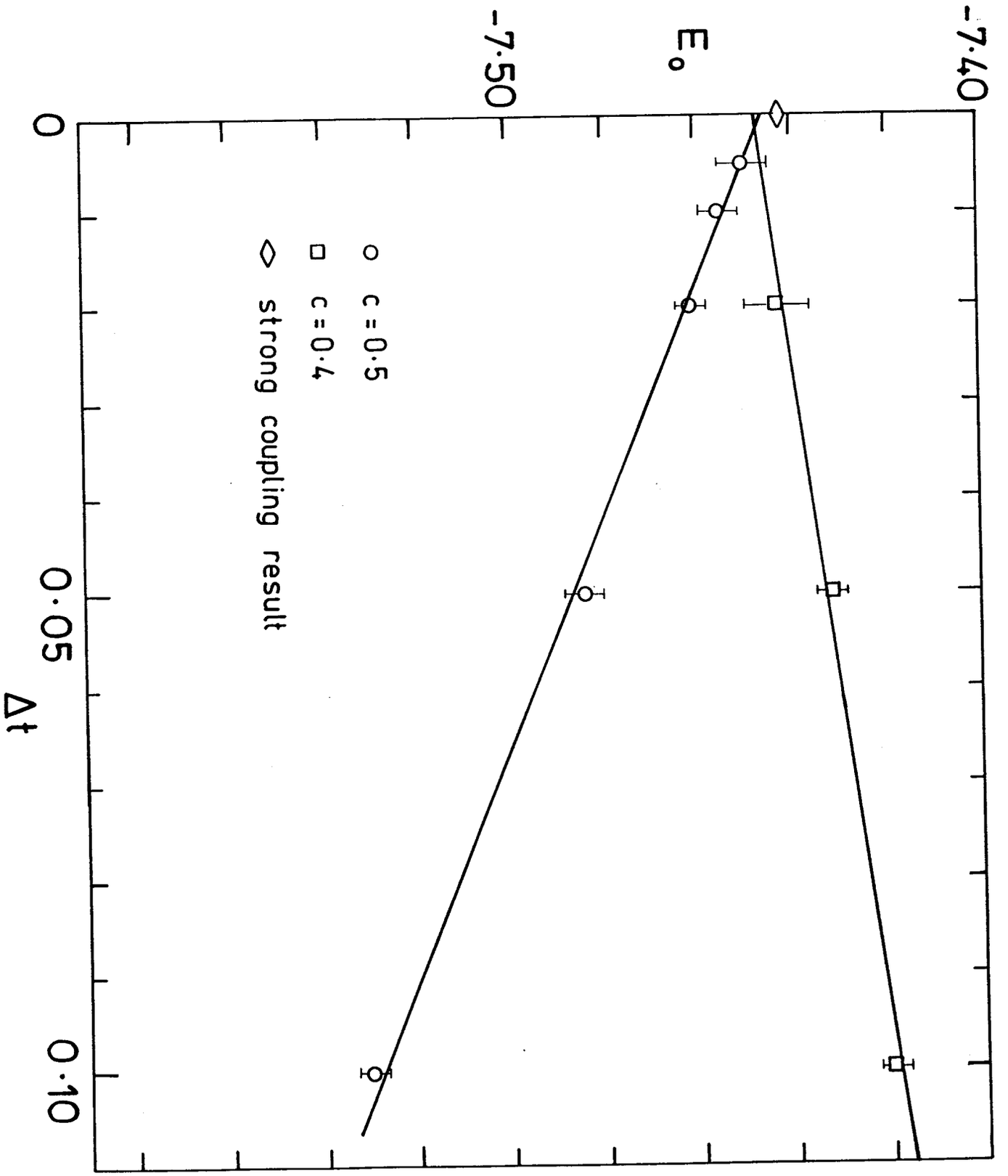

FIG. 1.

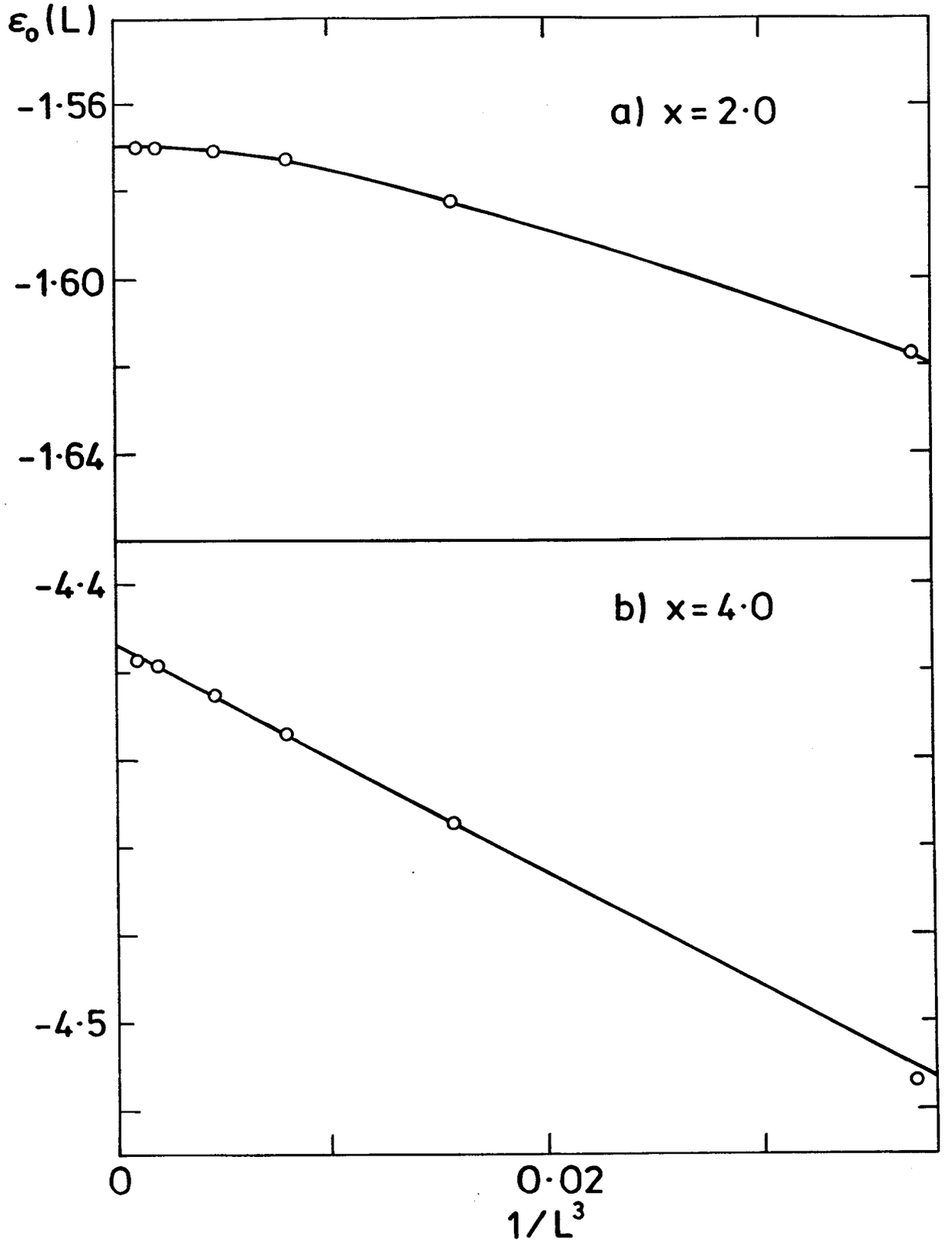

FIG. 2.

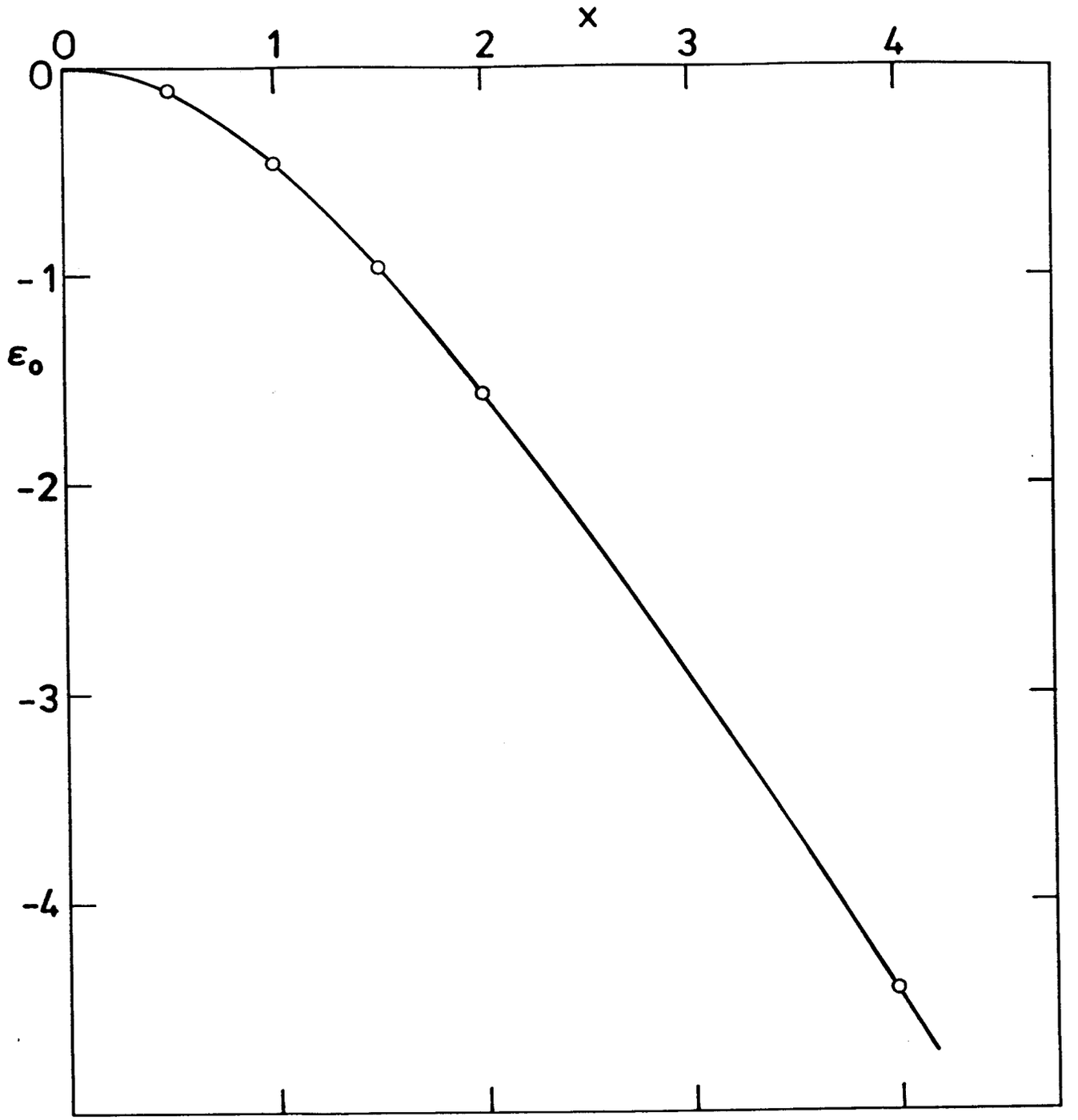

FIG. 3.

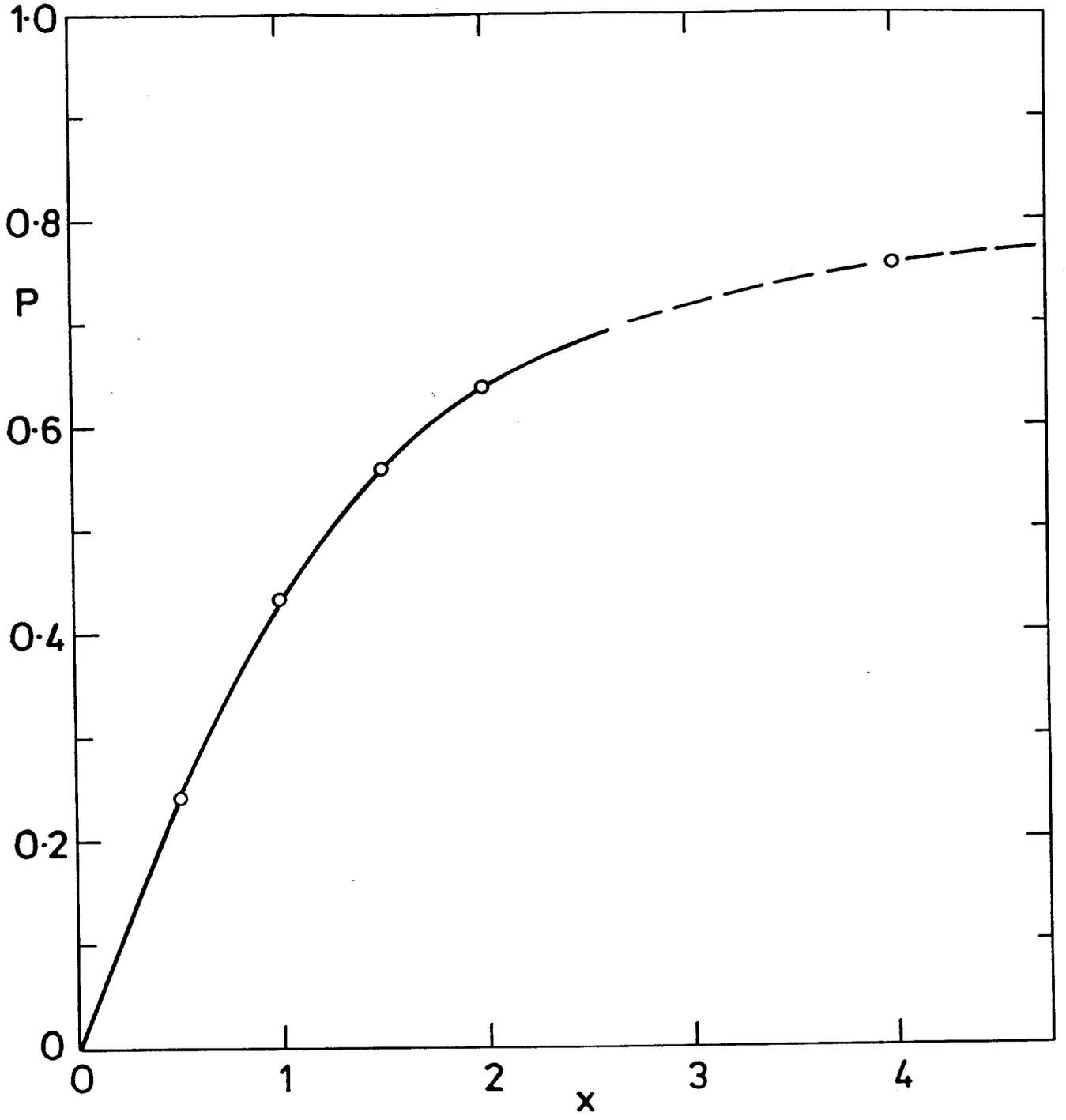

FIG. 4.

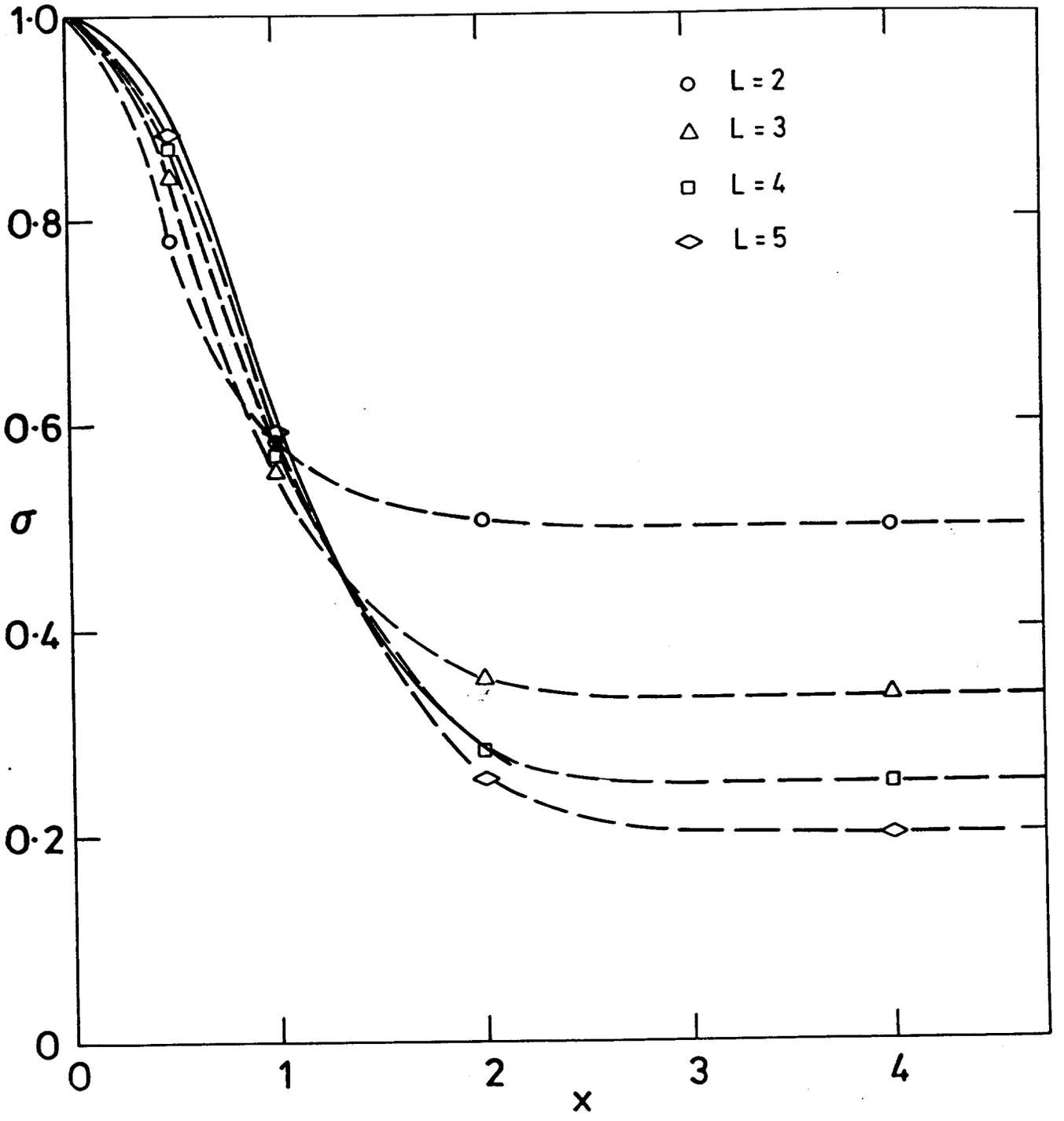

FIG. 5.

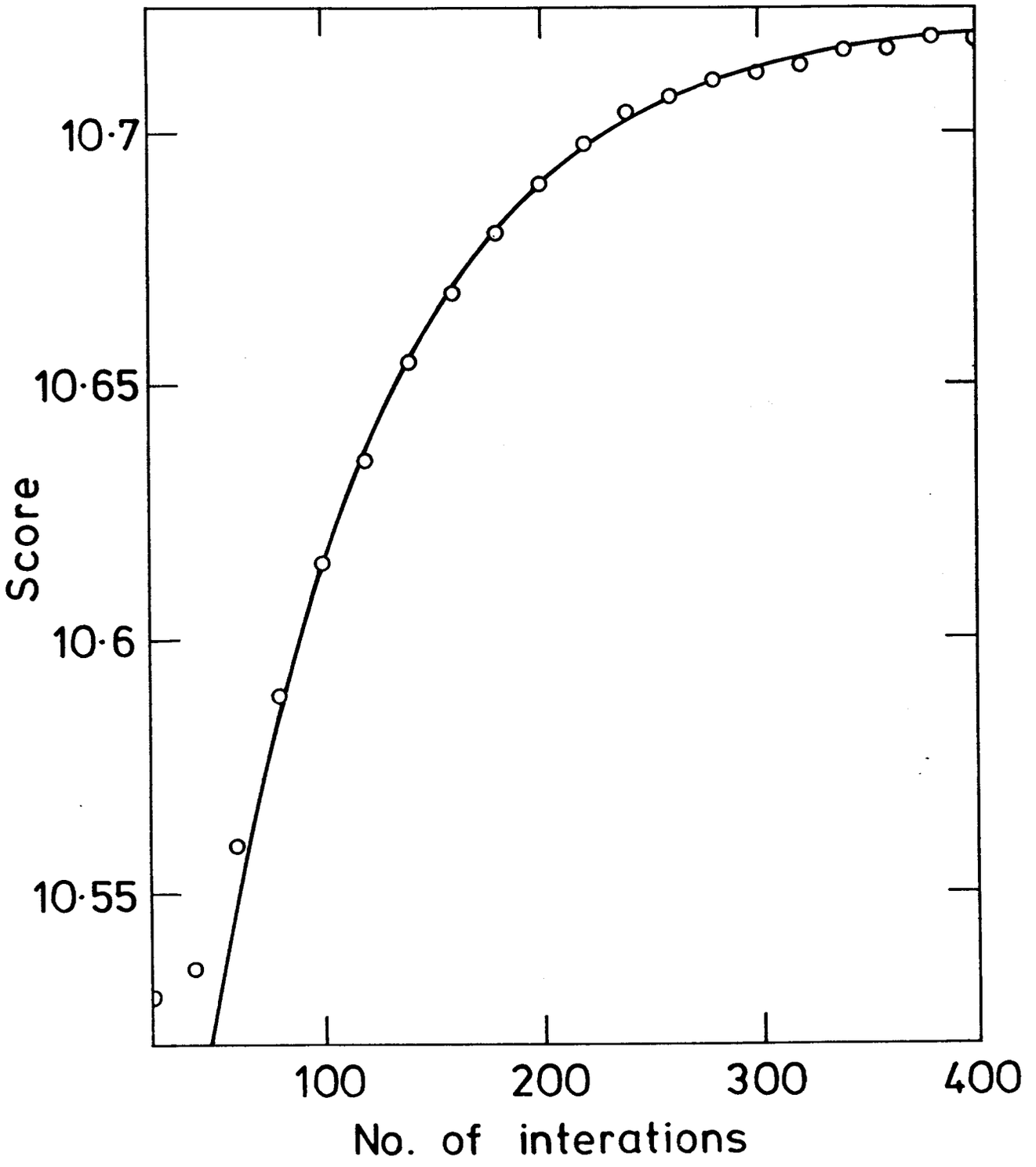

FIG. 6.